

# Simulation of Autothermal Reforming for Hydrogen Production

Sheeba Jilani<sup>1</sup> and Mohammad Hashim Khan<sup>2</sup>

<sup>1,2</sup>Department of Chemical Engineering, Aligarh Muslim University, Aligarh, India  
E-mail: <sup>1</sup>sheeba\_jilkani@yahoo.co.in

---

**Abstract**—Autothermal reforming is a most promising process for the hydrogen production from methane due to its neutral thermal behaviour. In this investigation, a one dimensional fixed bed catalytic autothermal reforming reactor is simulated numerically. A four reaction mechanism is implemented to model the reaction that occurs in the presence of Ni/Al<sub>2</sub>O<sub>3</sub> catalyst. The effects of some parameters (molar steam to carbon ratio and molar oxygen to carbon ratio) on the methane conversion and hydrogen yield are studied. Model is solved by finite difference method using MATLAB to select optimum values of these parameters which affects the process. The selected optimum values S/C of 6, O/C of 0.45, feed temperature of 500 °C and pressure of 1.5 bar gives the 98.3% methane conversion, 76.5 % hydrogen purity (on dry basis) and yield of 3.2 mole hydrogen per mole of methane supplied. Same model is solved at 1 atmospheric pressure to select the optimum range of molar S/C ratio and molar O/C ratio on same operating condition that gives the optimal range of molar S/C of 4-6 and molar O/C of 0.35-0.55 that gives the methane conversion greater than 84 %. The selected optimum value S/C of 5, O/C of 0.45, feed temperature of 500 °C and pressure of 1.0 atm gives the 98 % methane conversion, 76.5 % hydrogen purity (on dry basis) and yield of 3.3 mole hydrogen per mole of methane supplied.

## 1. INTRODUCTION

Meeting the growing energy demand, while keeping the environment clean is one of the most challenging issues facing the world in the 21<sup>st</sup> century. According to International Energy Reports, currently around 86% of the world's energy demand is satisfied with fossil fuels such as natural gas, coal, and petroleum. One promising alternative to fossil fuel is hydrogen, which can mitigate the problems of energy supply and the ill effects of hydrocarbons use. The reaction of hydrogen with oxygen can release energy explosively in heat engines and quietly in fuel cells to produce water as the by-product. Hydrogen is the current primary source of cheap energy that powers the modern industrial civilization. At the rate that oil and natural gas usage is going, known oil and fossil fuel reserves are not expected to last into the year 2038 [1].

The scientists define hydrogen as “the fuel for excellence”. Hydrogen has an important role to play in the future as an energy carrier for a clean energy in the world, as well as wide

applications in areas such as the production of chemicals, metallurgy and mostly at crude oil refining. Therefore, the demand of hydrogen has increased in recent time.

There are three major thermo-chemical reforming techniques used to produce hydrogen from hydrocarbon fuels, i.e. steam reforming (SR), partial oxidation (POX) and autothermal reforming (ATR).

Steam reforming (SR) is considered to be the most effective method of producing the highest hydrogen molar yield per mole of fuel. Steam reformers have been used for decades and can easily be scaled to any required size. The main drawback of steam reforming is that it is an endothermic process requiring the addition of heat to make the reaction proceed and this result in relatively low overall system efficiency.

Partial oxidation (POX) is a process where the overall reaction can be described as the reaction of a hydrocarbon fuel with oxygen over a catalytically active surface to produce hydrogen and carbon monoxide. The overall reaction is exothermic which eliminates the need for pre-heating compared with a basic steam reformer.

Autothermal reforming combines partial oxidation and steam reforming. Autothermal reforming (ATR) is a stand-alone process, in which the entire hydrocarbon conversion is completed in one reactor. Autothermal reforming is a process where fuel, air and steam are injected together over a catalytically active region where an oxidation reaction will occur followed by a steam reforming reaction. The oxidation reaction is highly exothermic and thus emits a large amount of heat. The elevated temperature promotes the reaction of the steam with the remaining fuel in a steam reforming reaction. The exothermic nature of POX and endothermic nature of SR make the overall reaction thermally neutral.

Trimm and Lam (1980) were among the first who studied ATR of methane. They measure ATR reaction kinetics on Pt/Al<sub>2</sub>O<sub>3</sub> fibre catalyst at temperatures around 800 K. This study

provided a description of the kinetics of methane oxidation on platinum supported on porous or non-porous alumina fibres.

Xu and Froment (1989) developed intrinsic kinetic for methane steam reforming, methanation, and water-gas shift reactions on Ni/Al<sub>2</sub>O<sub>3</sub> catalyst for initial temperature range among 573-823 K. This mechanism has been implemented in numerous investigations up to now.

Ma et al. (1996) designed and tested an autothermal reactor for the conversion of light hydrocarbon to hydrogen on Pt/ $\delta$ -Al<sub>2</sub>O<sub>3</sub> catalyst. They presented a kinetic rate equation for the reaction of methane total combustion based on this catalyst for initial temperature range of 663-723 K. The catalytic oxidation of methane, ethane and propane on a catalyst had been studied as part of the design of an autothermal reactor in which exothermic oxidation and endothermic steam reforming were combined.

Groote and Froment (1996) simulated the catalytic POX of methane to synthesis gas on a Ni catalyst in an adiabatic reactor with various inlet molar air to fuel (A/F) and molar water to fuel (W/F) ratios. The kinetic rates were presented for eight reactions and a series of effectiveness factors associated with these reactions were proposed.

Shukri et al. (2004) modelled a one-dimensional steady state adiabatic fixed bed reactor. In this study, effects of operating pressure, inlet temperature and steam to methane ratio were investigated. They showed that increase of steam to methane ratio over a certain value would decrease the methane conversion.

Hoang et al. (2005) studied kinetics and modelling of methane steam reforming over sulphide nickel catalyst on alumina support. Extensive experiments were carried out to study the performance of the steam reforming process and to determine its kinetic data. The results demonstrated that the reforming performance was strongly affected by temperature and ratio of steam to methane.

Amin et al. (2008) developed a one-dimensional mathematical model to simulate the performance of a catalytic fixed bed reactor for carbon dioxide reforming of methane over Rh/Al<sub>2</sub>O<sub>3</sub> at atmospheric pressure. The reactions involved in the system were carbon dioxide reforming of methane and reverse water gas shift reaction.

ZahediNezad et al. (2009) had kinetically modeled an autothermal reforming of methane in the presence of Ni/Mg-Al<sub>2</sub>O<sub>3</sub> catalyst. For kinetic modeling, reformer was divided in two sections, upper non-catalytic partial oxidation and lower catalytic steam reforming. They suggested that for feed conversion, 1700 K temperature was needed. Higher temperature increased the rate of reactions and reduced the timing of getting to equilibrium.

In the present study, catalytic ATR of methane in the presence of a Ni-based catalyst is numerically simulated. A one-dimensional, kinetic, heterogeneous, adiabatic model is developed. In this study, the effects of molar S/C ratio and molar O/C ratio on the methane conversion and hydrogen yield are studied.

## 2. AUTOTHERMAL REFORMING REACTOR MODEL

In this study, the packed bed autothermal reformer that has been analysed for hydrogen production operates on methane. This fuel along with steam and air are preheated using a furnace and mixed before being injected into the reactor inlet. The inlet stream then proceeds through porous Ni/Al<sub>2</sub>O<sub>3</sub> catalytic region so that a fully developed plug flow profile is achieved before the reactants reach the catalytically active porous region. In the presence of a catalyst (Ni/Al<sub>2</sub>O<sub>3</sub>), the inlet gas mixture chemically reacts to produce hydrogen, carbon monoxide, carbon dioxide, and steam. Nitrogen is also found in the product gas as it is present in the inlet air as well as trace amounts of unreacted fuel that did not achieve complete decomposition.

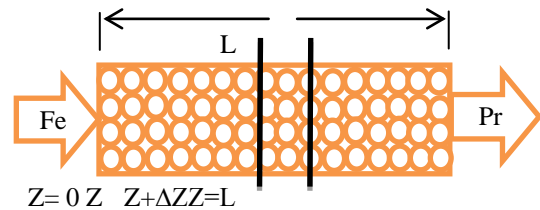


Fig. 1: Schematic diagram of a tubular packed bed autothermal reformer

## 3. CHEMICAL REACTION KINETICS

In this study, autothermal reforming (ATR) of methane is defined as the combination of partial oxidation (POX) and steam reforming (SR) under thermally neutral conditions and with consideration of no heat loss to the surroundings. In a catalytic reformer, there are many reactions taking place, whose rates depend strongly on the reforming conditions. To reduce the complexity in the development of a mathematical model, only the reactions with significant rates are considered. Based on chemical reactions in partial oxidation [8] and steam reforming of methane [25], one can easily come up with eight autothermal-related reactions, where the main ones include exothermic complete oxidation, followed by steam reforming, water-gas shift, and CO<sub>2</sub>-reforming reactions of methane. Other side reactions include cracking of methane and carbon monoxide to carbon deposition, and gasifying carbon by steam and oxygen. However, in these eight reactions, some reactions actually arrive from the combination of the others, while some have insignificantly low rates of reactions. For instance, the rate of direct CO<sub>2</sub> reforming is very small, much smaller than the complete oxidation and steam-reforming reactions, so it

can be ignored. The water gas shift reaction tends to influence the final H<sub>2</sub>/CO ratio depending on the feed steam to carbon ratio (S/C). At high operational temperature, the reaction will favour production of CO instead of H<sub>2</sub>; that is the reason why a large S/C ratio is used in methane reforming [17].

Thus, in an autothermal reformer, all reactions related to carbon deposition and carbon gasification can be ignored provided that the settings of oxygen to carbon ratio (O/C) and S/C are not too far away from the above mentioned. As a consequence, only four major reactions are considered in the model.

#### Partial Steam Reforming:

Partial Steam Reforming:



Total Steam Reforming:



Water Gas Shift:



Complete Oxidation:



#### 4. REACTION KINETIC MODEL

To reduce the complexity of the mathematical model development and solution, only the reactions with significant rates will be considered. Among the possible set of reactions previously discussed, the two steam reforming reactions R<sub>1</sub> and R<sub>2</sub>, water gas shift R<sub>3</sub>, and the complete oxidation reaction R<sub>4</sub> prove to have significant rates.

There is large number of kinetic models for steam reforming and water-gas shift reactions in literatures. The model of Xu and Froment (1989) over Ni-based catalyst is considered to be more general and has been extensively tested under lab-scale conditions [24]. It is investigated on a temperature range from 500 to 575 °C. The kinetic model of Trimm and Lam (1980) is considered as a rigorous study for methane combustion. The kinetic rate expression developed in their model at 557 °C is adopted for the methane combustion reaction in this work. However, since it was derived over supported Pt-based catalyst, the model adsorption parameters are adjusted for Ni-based catalyst [9]. The combined model for the kinetic rate equations of ATR is given below. The reaction equilibrium constants and Arrhenius kinetic parameters are listed in Table-1. Van't Hoff parameters for species adsorption are given in Table-3.

$$R_1 = \frac{k_1}{p_{\text{H}_2}^{2.5}} \left( p_{\text{CH}_4} * p_{\text{H}_2\text{O}} - \frac{p_{\text{H}_2}^3 * p_{\text{CO}}}{K_{\text{el}}} \right) * \frac{1}{Q_r^2} \quad (5)$$

$$R_2 = \frac{k_2}{p_{\text{H}_2}^{3.5}} \left( p_{\text{CH}_4} * p_{\text{H}_2\text{O}}^2 - \frac{p_{\text{H}_2}^4 * p_{\text{CO}_2}}{K_{\text{elII}}} \right) * \frac{1}{Q_r^2} \quad (6)$$

$$R_3 = \frac{k_3}{p_{\text{H}_2}} \left( p_{\text{CO}} * p_{\text{H}_2\text{O}} - \frac{p_{\text{H}_2} * p_{\text{CO}_2}}{K_{\text{elIII}}} \right) * \frac{1}{Q_r^2} \quad (7)$$

$$R_4 = \frac{k_4 * p_{\text{CH}_4} * p_{\text{O}_2}}{(1 + K_{\text{CH}_4}^c * p_{\text{CH}_4} + K_{\text{O}_2}^c * p_{\text{O}_2})^2} + \frac{k_4 * p_{\text{CH}_4} * p_{\text{O}_2}^{0.5}}{(1 + K_{\text{CH}_4}^c * p_{\text{CH}_4} + K_{\text{O}_2}^c * p_{\text{O}_2})} \quad (8)$$

$$Q_r = 1 + K_{\text{CO}} * p_{\text{CO}} + K_{\text{H}_2} * p_{\text{H}_2} + K_{\text{CH}_4} * p_{\text{CH}_4} + K_{\text{H}_2\text{O}} * \frac{p_{\text{H}_2\text{O}}}{p_{\text{H}_2}} \quad (9)$$

The rate of consumption or formation of an individual gas species based on the reactions in equation (1) - (4) is determined by summing up the reaction rates of that species in all four reactions. It should be noted that, to extract the kinetic data from a standard industrial catalyst pellet-filled reactor (other than fine catalyst powder used in laboratory), one has to consider the intra-particle mass transport limitations, which significantly reduce the reaction rates in the equation (5) - (8) with kinetic data shown in Tables 1–4. To account for this shortcoming, average reaction rates were suggested by Groote and Froment [1996]; these are determined by multiplying the rates (Eqs. (5) - (8)) with various effectiveness factors  $\eta_1=0.07$ ,  $\eta_2=0.06$ ,  $\eta_3=0.7$  and  $\eta_4=0.05$ , respectively. As a consequence, the conversion rate of the individual species is as follows:

$$r_{\text{CH}_4} = -\eta_1 * R_1 - \eta_2 * R_2 - \eta_4 * R_4 \quad \dots (10)$$

$$r_{\text{O}_2} = -2 * \eta_4 * R_4 \quad \dots (11)$$

$$r_{\text{CO}_2} = \eta_2 * R_2 + \eta_3 * R_3 + \eta_4 * R_4 \quad \dots (12)$$

$$r_{\text{H}_2\text{O}} = -\eta_1 * R_1 - 2 * \eta_2 * R_2 - \eta_3 * R_3 + 2 * \eta_4 * R_4 \quad (13)$$

$$r_{\text{H}_2} = 3 * \eta_1 * R_1 + 4 * \eta_2 * R_2 + \eta_3 * R_3 \quad (14)$$

$$r_{\text{CO}} = \eta_1 * R_1 - \eta_3 * R_3 \quad (15)$$

Table 1: Reaction equilibrium constants

|   | Equilibrium Constant, $K_{\text{ej}}$                                |
|---|----------------------------------------------------------------------|
| 1 | $K_{\text{el}} = \exp((-26830/T_s) + 30.114) \text{ (bar}^2\text{)}$ |
| 2 | $K_{\text{elII}} = K_{\text{elII}} * K_{\text{elIII}}$               |
| 3 | $K_{\text{elIII}} = \exp((4400/T_s) - 4.036) \text{ (bar}^2\text{)}$ |

Table 2: Arrhenius kinetic parameters

| j | $k_{\text{oj}} \text{ (mol/Kg}_{\text{cat}}\text{.s)}$ | $E_j \text{ (J/mol)}$ |
|---|--------------------------------------------------------|-----------------------|
| 1 | $1.17 \times 10^{15} \text{ bar}^{0.5}$                | 2,40,100              |

|    |                                         |          |
|----|-----------------------------------------|----------|
| 2  | $2.83 \times 10^{14} \text{ bar}^{0.5}$ | 2,43,900 |
| 3  | $5.43 \times 10^5 \text{ bar}^{-1}$     | 67,130   |
| 4a | $8.11 \times 10^5 \text{ bar}^{-2}$     | 86,000   |
| 4b | $6.82 \times 10^5 \text{ bar}^{-2}$     | 86,000   |

**Table 3: Van't Hoff parameters for species adsorption**

| i                | $K_{oi}(\text{bar}^{-1})$      | $\Delta H_i(\text{J/mol})$ |
|------------------|--------------------------------|----------------------------|
| CH <sub>4</sub>  | $6.65 \times 10^{-4}$          | -38,280                    |
| CO               | $8.23 \times 10^{-5}$          | -70,650                    |
| H <sub>2</sub>   | $6.12 \times 10^{-9}$          | -82,900                    |
| H <sub>2</sub> O | $1.77 \times 10^5 \text{ bar}$ | 88,680                     |

**Table 4: Van't Hoff parameters for species combustion**

| i               | $K_{oi}^c(\text{bar}^{-1})$ | $\Delta H_i^c(\text{J/mol})$ |
|-----------------|-----------------------------|------------------------------|
| CH <sub>4</sub> | $1.26 \times 10^{-1}$       | -27300                       |
| O <sub>2</sub>  | $7.78 \times 10^{-7}$       | -92800                       |

## 5. REFORMER MODELING

A 1-D heterogeneous model is constructed to investigate the autothermal reforming (ATR) process behaviour on Ni/Al<sub>2</sub>O<sub>3</sub> catalyst at dynamic conditions in a fixed bed reformer.

**Modeling Assumptions:** The major assumptions in the model can be listed as follows:

1. Gases are assumed to obey the ideal gas law ;
2. Outer walls are well insulated and therefore assumed adiabatic operation;
3. Mass axially dispersed plug-flow conditions are considered with negligible radial gradients;
4. Catalyst deactivation has been neglected ;
5. Thermal radiation is not considered
6. Thermal dispersion in the axial direction is also considered with negligible radial gradients;
7. Concentration and temp. gradients in the radial direction are ignored;
8. Six reactive species (CH<sub>4</sub>, O<sub>2</sub>, CO, CO<sub>2</sub>, H<sub>2</sub>, H<sub>2</sub>O) and one inert component (N<sub>2</sub>) are involved in the model;
9. Uniform particle size;
10. Bed porosity is constant in the axial and radial bed directions

## 6. MASS BALANCES

General form of mass balance, in terms of volumetric concentration, for gaseous & solid phase respectively, is:

$$\varepsilon_b * \frac{\partial C_i}{\partial t} = \varepsilon_b * D_z * \frac{\partial^2 C_i}{\partial z^2} - \frac{\partial(u.C_i)}{\partial z} - k_{g,i} * A_C * (C_i - C_{i,s}) \quad (16)$$

$$(1 - \varepsilon_b) * \frac{\partial C_{i,s}}{\partial t} = k_{g,i} * A_C * (C_i - C_{i,s}) + (1 - \varepsilon_b) * \rho_{cat} * r_i \quad (17)$$

Rate of accumulation of the concentration in the solid particle (C<sub>i,s</sub>) is ignored, due to small particle size, see [Reid et al, 1988]

So equation (17) becomes:

$$k_{g,i} * A_C * (C_i - C_{i,s}) = -(1 - \varepsilon_b) * \rho_{cat} * r_i \quad (18)$$

So, we get the final general form of mass balance equation:

$$\varepsilon_b * \frac{\partial C_i}{\partial t} = \varepsilon_b * D_z * \frac{\partial^2 C_i}{\partial z^2} - \frac{\partial(u.C_i)}{\partial z} + (1 - \varepsilon_b) * \rho_{cat} * r_i \quad (19)$$

where, i indicated the progressive number of the chemical specie; all the other symbols are shown in the nomenclature at the end of this document.

## 7. ENERGY BALANCES

General form of energy balance for gaseous & solid phases respectively:

$$\varepsilon_b * \rho_f * C_{p,g} * \frac{\partial T_g}{\partial t} = -u * \rho_f * C_{p,g} * \frac{\partial T_g}{\partial z} + h_f * A_C * (T_s - T_g) + \lambda_z^f * \frac{\partial^2 T_g}{\partial z^2} \quad (20)$$

$$\rho_{bed} * C_{p,bed} * \frac{\partial T_s}{\partial t} = -h_f * A_C * (T_s - T_g) + \rho_{cat} * (1 - \varepsilon_b) * \sum_j^4 -\Delta H_{rxn,j} * \eta_i * R_j \quad (21)$$

where, j is the progressive number of investigated chemical reactions.

## 8. INITIAL AND BOUNDARY CONDITIONS

The proposed mathematical model is a system of 9 partial differential equations (PDE) with variable coefficients (7 are mass balances for the seven chemical species and two for the energy balance of solid and gaseous phases); so the problem is resolved only when the relative initial and boundary conditions are established.

**Initial condition:**  $t=0$ ;

$$C_i = C_{i,o}; T_i = T_o; C_{i,s} = C_{i,s,o}$$

**Boundary conditions:**

$$\text{At the reformer inlet, } z=0; \quad C_i = C_{i,o}; T_i = T_o; C_{i,s} = C_{i,s,o}; \quad P = P_o$$

At the reformer exit,  $z=L$ ;

$$\frac{\partial C_i}{\partial z} = 0; \frac{\partial T_g}{\partial z} = 0; \frac{\partial T_s}{\partial z} = 0;$$

## 9. ANALYSIS OF PRESSURE DROP

For the analysis of pressure drop in fixed bed reactor, Ergun equation is used [Ergun, 1952], it is equal to:

$$\frac{\partial P}{\partial z} = -K_D * u - K_V * u^2$$

$K_D$  and  $K_V$  are parameters corresponding to the viscous and kinetic loss terms, respectively, and described by semi-empirical relation as:

$$K_D = \frac{150 * \mu_g * (1 - \epsilon_b)^2}{d_p^2 * \epsilon_b^3}$$

$$K_V = \frac{1.75 * (1 - \epsilon_b) * \rho_f}{d_p * \epsilon_b^3}$$

## 10. OTHER GOVERNING EQUATIONS

The axial dispersion coefficient to account for the non-ideal flow and local mixing at turbulent velocities plus the diffusive flow is estimated using the equation of Edwards and Richardson (1968), [13]

$$D_z = 0.73 * D_m + \frac{0.5 * u * d_p}{1 + 9.49 * (D_m / u * d_p)} \quad \dots (25)$$

The axial thermal effective conductivity of the bed is determined from the correlation given in Yagi et al. (1960), [26]

$$\lambda_z^f / \lambda_g = \lambda_z^{f,0} / \lambda_g + 0.75 * Pr * Re \quad (26)$$

Where,

$$\frac{\lambda_z^{f,0}}{\lambda_g} = \epsilon_b + \frac{(1 - \epsilon_b)}{0.139 * \epsilon_b - 0.0339 + (2/3) * (\lambda_g / \lambda_s)}$$

The heat transfer coefficient,  $h_f$ , is also determined from the Chilton–Colburn factor,  $j_H$  [15]. The transport coefficients are presented as follows:

$$h_f = j_H * \frac{C_{p,g} * G_s}{Pr^{2/3}} \quad \dots (27)$$

If  $0.01 < Re < 50$ ,

$$j_H = 0.91 * Re^{-0.51} * \psi$$

If  $50 < Re < 1000$ ,

$$j_H = 0.61 * Re^{-0.41} * \psi$$

Where,  $\psi$  is a coefficient depending on the particle shape; for spherical particle  $\psi$  has a value of 1.

The dimensionless numbers used in the calculation are as follows:

Reynolds Number:

$$Re = \frac{(\rho_f * u * d_p)}{\mu_g} \quad (28)$$

Prandtl Number:

$$\dots (29) = \frac{(C_{p,g} * \mu_g)}{\lambda_g} \quad (29)$$

As the temperature changes the change in reaction enthalpy also changes, so the change in enthalpy is calculated by:

$$\Delta H_{new} = \Delta H_{298K} - C_p * dT \quad (30)$$

## 11. SOLUTION PROCEDURE:

This theoretical work deals with the dynamic analysis of autothermal reforming reactor (ATR). The mathematical model used for ATR consists of a set of 9 partial differential equations (eq. 3.26-3.34) (7 PDEs for component balance & 2 PDEs for energy balance). The component balance equations contains rate of reaction terms for each component. For the simulation of ATR, the model equations are solved using the finite difference method in MATLAB R2011b. This method is used as a spatial discretization method over a uniform grid of 50 intervals.

The operating conditions combined with initial conditions have been listed in table 5 & 6 which is taken from Halabi et al. (2009). These operating and initial conditions used for solving the model to investigate the fuel conversion and  $H_2$  yield.

Table 5: Reactor parameters & operating conditions

| Parameter                    | Value                | Unit                   |
|------------------------------|----------------------|------------------------|
| Reactor Length               | 0.4                  | m                      |
| Gas Feed Temperature         | 500                  | °C                     |
| Catalyst Temperature         | 500                  | °C                     |
| Pressure                     | 1.5                  | Bar                    |
| Catalyst Density             | 1870                 | Kg/m <sup>3</sup>      |
| Bed Void Fraction            | 0.4                  | -                      |
| Catalyst Particle Diameter   | 2 x 10 <sup>-3</sup> | m                      |
| Gas Mass Flow Velocity       | 0.15                 | Kg/(m <sup>2</sup> .s) |
| Steam to Carbon Molar Ratio  | 6                    | -                      |
| Oxygen to Carbon Molar Ratio | 0.45                 | -                      |

Table 6: Average gas properties

| Parameter                  | Value                    | Unit              |
|----------------------------|--------------------------|-------------------|
| Molecular diffusivity      | 1.6 x 10 <sup>-5</sup>   | m <sup>2</sup> /s |
| Gas Viscosity              | 0.031 x 10 <sup>-3</sup> | Kg/(m.s)          |
| Gas Thermal Conductivity   | 0.0532                   | W/(m.K)           |
| Solid Thermal Conductivity | 13.8                     | W/(m.K)           |
| Bed Heat Capacity          | 850                      | J/(kg.K)          |
| Universal Gas Constant     | 8.314                    | J/mol.K           |

## 12. SIMULATION RESULTS

### 12.1 Result Validation

Solving the model at given initial and operating conditions, high rate of CH<sub>4</sub> conversion & highest purity H<sub>2</sub> is achieved.

In Fig. -2, the steady state dry concentration profile showed along with the relative reformer length. In this Fig. it can be seen the concentration change of different species (on dry basis). The product contains 3.2 mole of H<sub>2</sub> per mole of CH<sub>4</sub> fed and the CH<sub>4</sub> conversion of 98.3 %.

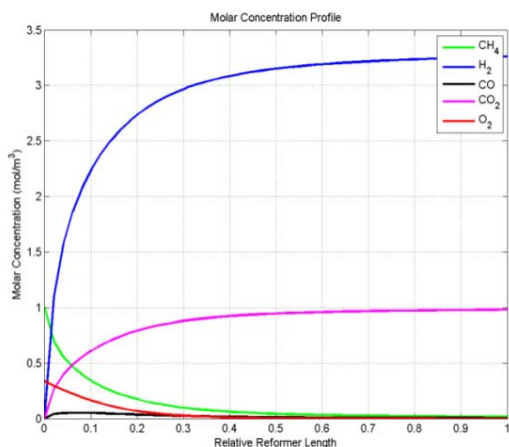


Fig. 2: Dry concentration profile at P=1.5 bar, O/C = 0.45, S/C=6 & feed T=773.15 K

The result is validated with the work of Halabiet. al. (2009), they get the yield of 2.6 moles H<sub>2</sub> per mole of CH<sub>4</sub> and in this work 3.2 moles of H<sub>2</sub> per mole of CH<sub>4</sub> is achieved. They obtained a conversion of 93% and H<sub>2</sub> purity & yield of 73% and 2.6 respectively and this study gives the conversion of 98.3% and H<sub>2</sub> purity & yield of 76.5% and 3.2, respectively.

Table 7: Validation of result of ATR for O/C=0.45 & S/C=6 at P=1.5 bar & T=773.15 K

|                                    | Halabi et al. | Simulation Result |
|------------------------------------|---------------|-------------------|
| <b>Conversion (%)</b>              | 93            | 98.3              |
| <b>Purity (%)</b>                  | 73            | 76.5              |
| <b>Yield</b>                       | 2.6           | 3.2               |
| <b>Equilibrium Temperature (K)</b> | 862           | 828               |
| <b>Steady State Timing</b>         | 13 Minute     | 10 Minute         |

### 13. RESULTS AT ATMOSPHERIC PRESSURE:

After the validation, the model is solved for the same operating conditions at 1 atmospheric pressure for different initial feed ratios to select an optimum feed condition.

Fig. -3 shows the CH<sub>4</sub> conversion profile for different O/C and S/C molar ratios at 1 atm pressure and feed temperature of 773.15 K. From the Fig. it can be selected the molar ratios O/C and S/C for higher conversion of CH<sub>4</sub>. In this Fig. it can be seen that the highest conversion attained by the molar ratios O/C=0.55 and S/C=4.5, that is almost 100%. Practically it is impossible to get total conversion, so it has to be select an optimum molar ratio of O/C and S/C. The lower O/C ratios (i.e. 0.35 & 0.45) have low conversion, but the conversion slightly increases with the increasing O/C values. From this Fig. the ratios O/C=0.45 & S/C=5 have the optimum conversion of 98%.

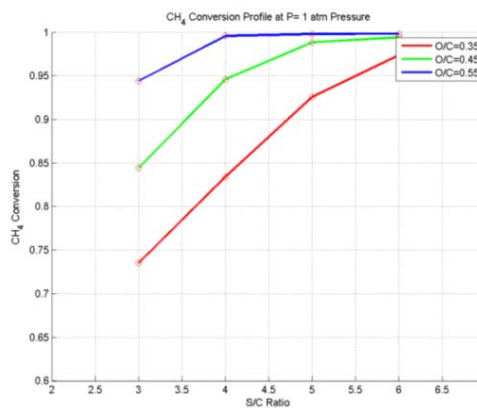
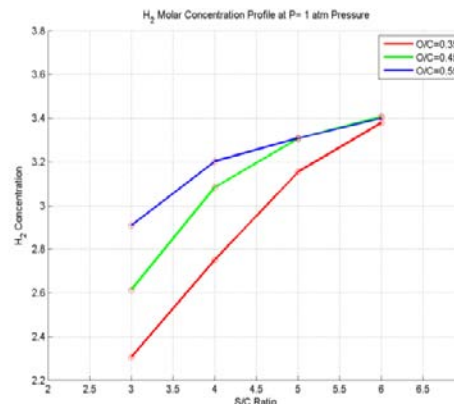


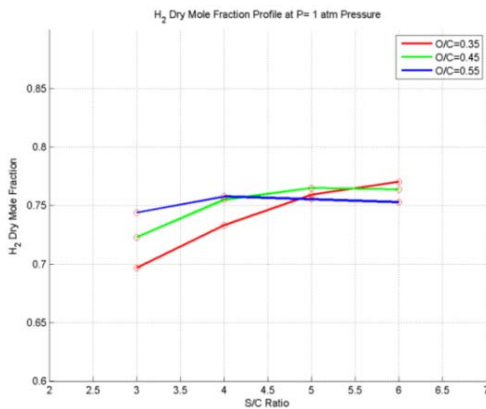
Fig. 3: CH<sub>4</sub> conversion profile for different O/C & S/C at P=1atm and feed T=773.15 K

Fig. -4 shows the number of moles of H<sub>2</sub> produced per 1 mole of CH<sub>4</sub> supplied, under different O/C and S/C ratios at P=1 atm and a feed temperature T=773.15 K. As can be seen from Fig. 4.12, the highest mole number of H<sub>2</sub> produced per 1 mole of CH<sub>4</sub> supplied is 3.4 at O/C of 0.45, 0.55 and S/C of 6, i.e., 1 mol of CH<sub>4</sub> supplied can produce 3.4 mol of H<sub>2</sub>. But it has to select the optimum value that gives best results at low reactant consumption. So, the selected value is O/C=0.45 & S/C=5, that gives the yield of 3.3 mol of H<sub>2</sub> per mole of CH<sub>4</sub> supplied.



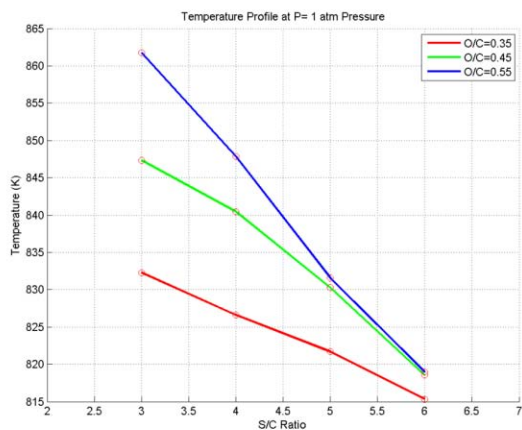
**Fig. 4:** Moles of  $H_2$  produced per 1 mole of  $CH_4$  fed at different O/C & S/C at  $P=1$  atm and feed  $T=773.15$

Fig. -5 shows  $H_2$  product purity at different O/C and S/C molar ratios for 1 atm pressure. From the Fig. it is clear that highest purity  $H_2$  is produced at O/C=0.35 and S/C=6, which is 77%. But the ratio of O/C=0.45 and S/C=5 gives the purity of  $H_2$  is 76.5%, which is not much less than highest purity. So, the molar ratios O/C=0.45 and S/C=5 for optimum result is selected.



**Fig. 5:** Dry mole-fraction of  $H_2$  at different O/C & S/C at  $P=1$  atm and feed  $T=773.15$  K

Fig. -6 presents the variation of the product temperature at  $P=1$  atm and feed temperature  $T=773.15$  K under different O/C and S/C ratios. Results show that for a fixed S/C, the temperature increases with the increase of O/C. Contrarily, for a fixed O/C, the increase in S/C leads to decreasing product temperature. This is due to the increase in exothermic oxidation when increasing O/C, but an increase in endothermic steam-reforming reaction when increasing S/C.



**Fig. 6:** Product temperature profile at different O/C & S/C at  $P=1$  atm & feed  $T=773.15$  K

Selected optimum molar ratio O/C=0.45 and S/C= 5 gives molar concentration of  $H_2$  product is 3.3 mole per mole of  $CH_4$  fed as shown in Fig. -7. The conversion of  $CH_4$  is 98%.

In this Fig. it can be seen that 1 mole of  $CH_4$  produces 3.3 mole of  $H_2$ .

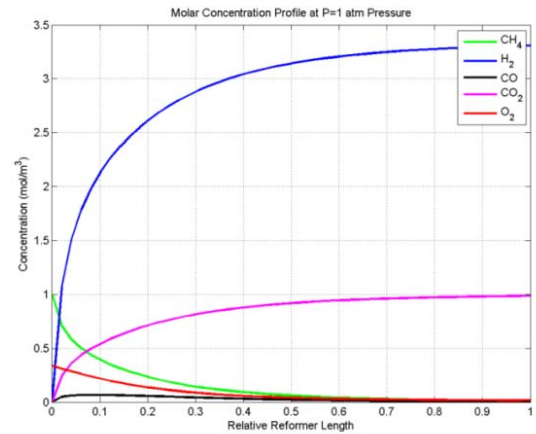


**Fig. 7:** Dry concentration profile for O/C= 0.45, S/C=5 at  $P=1$  atm and feed temperature  $T=773.15$  K

The steady-state equilibrium composition profiles (i.e. mole fraction profiles) of the gas species on dry basis as a function of the axial reactor coordinate are given in Fig. -8. The  $H_2$  purity obtained at the S/C ratio of 5, and O/C ratio of 0.45 is 76.5% with corresponding  $CH_4$  conversion of 98%,  $H_2$  yield of 3.3 mole  $H_2$  produced/mole  $CH_4$  fed.

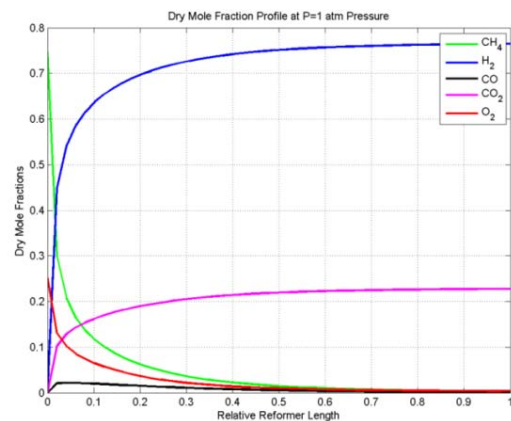


**Fig. 9:** Steady state composition profile (on dry basis) for O/C=0.45 & S/C=5 at  $P=1$  atm and feed temperature  $T=773.15$  K

The temperature is changing with time until it approaches steady state conditions at 831 K in about 9 min with a maximum rise of  $58^\circ\text{C}$  above the feed inlet temperature. Fig. -8 shows the temperature profiles along the reformer length at steady state in the gas and solid phases. Both profiles are almost identical throughout the reformer length.

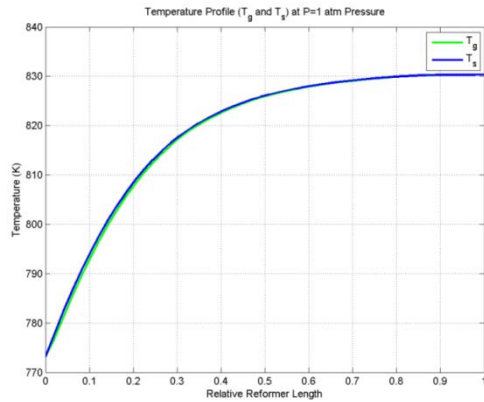


Fig. 8: Temperature profile of bulk gas and solid catalyst for O/C=0.45, S/C=5 at P= 1atm and feed temperature T =773.15 K

## 14. CONCLUSION

In this work a one dimensional non-isothermal mathematical model is taken to analyse the dynamic performance of catalytic autothermal reformer (ATR). The catalyst used in the reactor is Ni/Al<sub>2</sub>O<sub>3</sub>. The performance of ATR is basically depends on the initial feed conditions that are O/C and S/C ratio. The model is solved for the operating and initial feed conditions suggested by Halabi et al (2009). The performance of ATR is validated with the work of Halabi et al. (2009). The simulation results show that the conversion of CH<sub>4</sub> is very high. The reaction approaches to steady state condition (thermal equilibrium) in 10 minutes with a conversion of 98.3% and H<sub>2</sub> purity & yield of 76.5% and 3.2, respectively.

Same model is solved at atmospheric pressure for selecting the optimum initial feed ratios of O/C & S/C ratios at 1 atm pressure. From the result, an optimum ratios of O/C= 0.45 & S/C=5 at 773.15 K feed temperature are selected. From this ratio it can be seen that CH<sub>4</sub> conversion of 98% and H<sub>2</sub> purity & yield of 76.5% and 3.3, respectively.

In high temperature systems, radiation heat transfer plays a significant role. For future work, considering the radiation effects could improve the result. Also, the heat transfer coefficient could be found out as a function of local Reynolds number. Specifically, in the ATR evaluation, combustion could be modelled to include its turbulent effects.

Finally, there is a possibility of incorporating the 1-D model in a 2-D model, such as honey comb structure which could lead to better design and thermal management.

## 15. NOMENCLATURE

A<sub>c</sub> External catalyst surface area per unit volume of catalyst bed (m<sup>2</sup>/m<sup>3</sup>)

|                              |                                                                                                  |                     |                   |
|------------------------------|--------------------------------------------------------------------------------------------------|---------------------|-------------------|
| C <sub>i</sub>               | Concentration of species <i>i</i> in the (mol/m <sup>3</sup> )                                   | gas                 | phase             |
| C <sub>i,s</sub>             | Concentration of species <i>i</i> in the (mol/m <sup>3</sup> )                                   | solid               | phase             |
| C <sub>p,bed</sub>           | Specific heat of the catalyst bed                                                                | (J/(kg K))          |                   |
| C <sub>pg</sub>              | Specific heat of the fluid (J/(kg K))                                                            |                     |                   |
| D <sub>i</sub>               | Effective diffusion coefficient                                                                  | (m <sup>2</sup> /s) |                   |
| D <sub>m</sub>               | Average molecular diffusivity                                                                    | (m <sup>2</sup> /s) |                   |
| D <sub>z</sub>               | Axial dispersion coefficient (m <sup>2</sup> /s)                                                 |                     |                   |
| d <sub>p</sub>               | Catalyst particle diameter (m)                                                                   |                     |                   |
| E <sub>j</sub>               | Activation energy of reaction <i>j</i>                                                           | (J/mol)             |                   |
| G <sub>s</sub>               | Gas mass flow velocity (kg/(m <sup>2</sup> s))                                                   |                     |                   |
| ΔH <sub>i</sub>              | Heat of adsorption of species <i>i</i>                                                           | (J/mol)             |                   |
| ΔH <sub>i</sub> <sup>c</sup> | Heat of adsorption of combusting species <i>i</i>                                                | (J/mol)             |                   |
| ΔH <sub>298K</sub>           | Heat of reaction of at STP (kJ/mol)                                                              |                     |                   |
| h <sub>f</sub>               | Gas to solid heat transfer coefficient (W/(m <sup>2</sup> s))                                    |                     |                   |
| j <sub>D</sub>               | Chilton–colburn factor for mass transfer                                                         |                     |                   |
| j <sub>H</sub>               | Chilton–colburn factor for heat transfer                                                         |                     |                   |
| k <sub>g,i</sub>             | Gas to solid mass transfer coefficient of component <i>i</i> (m <sup>3</sup> /m <sup>2</sup> .s) |                     |                   |
| k <sub>j</sub>               | Temperature dependent kinetic rate constant of reaction <i>j</i>                                 |                     |                   |
| k <sub>oj</sub>              | Reference temperature dependent kinetic rate constant of reaction <i>j</i>                       |                     |                   |
| K <sub>j</sub>               | Thermodynamic equilibrium constant of reaction <i>j</i>                                          |                     |                   |
| K <sub>oi</sub>              | Reference adsorption constant of species <i>i</i>                                                |                     |                   |
| K <sub>i</sub>               | Adsorption constant of species <i>i</i>                                                          |                     |                   |
| K <sub>oi</sub> <sup>c</sup> | Reference adsorption constant of combusting species <i>i</i>                                     |                     |                   |
| K <sub>i</sub> <sup>c</sup>  | Adsorption constant of combusting species <i>i</i>                                               |                     |                   |
| K <sub>D</sub>               | Parameter corresponding to the (Pa.s/m <sup>2</sup> )                                            |                     | viscous loss term |
| K <sub>V</sub>               | Parameter corresponding to the (Pa.s <sup>2</sup> /m <sup>3</sup> )                              |                     | kinetic loss term |
| p <sub>i</sub>               | Partial pressure of gas species <i>i</i>                                                         | (bar)               |                   |
| P                            | Total gas pressure (bar)                                                                         |                     |                   |
| Pr                           | Prandtl number                                                                                   |                     |                   |
| r <sub>i</sub>               | Rate of consumption or formation of species <i>i</i> (mol/(kgcat.s))                             |                     |                   |
| R <sub>j</sub>               | Rate of reaction <i>j</i> (mol/(kgcat.s))                                                        |                     |                   |
| R                            | Universal gas constant (J/mol K)                                                                 |                     |                   |
| Re                           | Reynolds number                                                                                  |                     |                   |
| Sc <sub>i</sub>              | Schmitt number                                                                                   |                     |                   |
| T                            | Gas phase temperature (K)                                                                        |                     |                   |
| T <sub>s</sub>               | Solid catalyst temperature (K)                                                                   |                     |                   |
| t                            | Time (s)                                                                                         |                     |                   |
| u                            | Superficial gas flow velocity (m/s)                                                              |                     |                   |
| u <sub>inst</sub>            | Interstitial gas velocity (m/s)                                                                  |                     |                   |
| Y <sub>i</sub>               | Dry mole fraction of species <i>i</i>                                                            | (mol/mol)           |                   |
| z                            | Axial dimension (m)                                                                              |                     |                   |

## 16. GREEK LETTERS

|                |                                         |
|----------------|-----------------------------------------|
| Ω              | Dominator term in the reaction kinetics |
| ε <sub>b</sub> | Packing bed porosity                    |
| η <sub>j</sub> | Effectiveness factor of reaction        |

|               |                                                            |                      |
|---------------|------------------------------------------------------------|----------------------|
| $\lambda_g$   | Average gas thermal conductivity                           | (W/m K)              |
| $\lambda_s$   | Solid thermal conductivity                                 | (W/m K)              |
| $\lambda_z^f$ | Effective thermal conductivity                             | (W/m K)              |
| $\mu_g$       | Average gas viscosity                                      | (kg/(m.s))           |
| $\rho_{bed}$  | Density of the catalyst bed                                | (kg/m <sup>3</sup> ) |
| $\rho_{cat}$  | Density of the catalyst pellet                             | (kg/m <sup>3</sup> ) |
| $\rho_f$      | Density of the fluid                                       | (kg/m <sup>3</sup> ) |
| $\Psi$        | Particle shape factor (for spherical particles, $\Psi=1$ ) |                      |

## REFERENCES

- [1] Ahmed S., Krumpelt M., "Hydrogen from hydrocarbon fuels for fuel cells", *Int. J. Hydrogen Energy*, Vol. 26 (2001): 291–301.
- [2] Akpan E., Sun Y., Kumar P., Ibrahim H., Aboudheir A., Idem R., "Kinetics, experimental and reactor modelling studies of the carbon dioxide reforming of methane (CDRM) over a new Ni/CeO<sub>2</sub>-ZrO<sub>2</sub> catalyst in a packed bed tubular reactor". *Chem. Eng. Sci.*, Vol. 62 (2007): 4012-4024.
- [3] Biesheuvel P.M., Kramer G.J., "Two-section model for autothermal reforming of methane to synthesis gas", *AIChE J.*, Vol. 49 (2003): 1827–1837.
- [4] Bird R.B., Stewart W.E., Lightfoot E.N., "Transport Phenomena", second ed., Wiley, New York, 2002.
- [5] Blanks R.F., Wittrig T.S. and Peterson D.A., "Bidirectional adiabatic synthesis gas generator", *Chem. Eng. Sci.*, Vol. 45 (1990): 2407-2413.
- [6] Chan S.H., Wang H.M., "Thermodynamic analysis of natural gas fuel processing for fuel cell applications", *Int. J. Hydrogen Energy*, Vol. 25 (2000): 441–449.
- [7] Chan S.H., Wang H.M., "Carbon monoxide yield in natural gas autothermal reforming process", *J. Power Sources*, Vol. 101 (2001): 188–195.
- [8] De Groote A.M., Froment G.F., "Simulation of the catalytic partial oxidation of methane to synthesis gas", *Appl. Catal. A*, Vol. 138 (1996): 245–264.
- [9] De Smet C.R.H., De Croon M.H.J.M., Berger R.J., Marin G.B., Schouten J.C., "Design of adiabatic fixed-bed reactors for the partial oxidation of methane to synthesis gas. Application to production of methanol and hydrogen-for-fuel-cells", *Chem. Eng. Sci.*, Vol. 56 (2001): 4849–4861.
- [10] De Wash A.P., Froment G.F., "Heat transfer in packed bed", *Chem. Eng. Sci.*, Vol. 27 (1972): 567–576.
- [11] Ding Y., Alpay E., Adsorption-enhanced steam-methane reforming, *Chem. Eng. Sci.* Vol. 55 (2000): 3929–3940.
- [12] Edwards M.F., Richardson J.F., Gas dispersion in packed beds, *Chem. Eng. Sci.*, Vol. 23 (1968): 109–123.
- [13] Ergun S., Fluid flow through packed columns, *Chem. Eng. Prog.*, Vol. 48 (1952): 89–94.
- [14] Froment G.F., Bischoff K.B., "Chemical Reactor Analysis and Design", 3<sup>rd</sup> ed., Wiley, New York, 2011.
- [15] Geankoplis C.J., "Transport Processes and Unit Operations", 3<sup>rd</sup> ed., Prentice Hall Int., 1993.
- [16] Halabi M.H., De Croon M.H.J.M., Vander Schaaf J., Cobden P.D., Schouten J.C. "Modeling and analysis of autothermal reforming of methane to hydrogen in a fixed bed reformer", *Chem. Eng. J.*, Vol. 137 (2008): 568-578.
- [17] Hoang D.L., Chan S.H., "Modeling of a catalytic autothermal methane reformer for fuel cell applications", *Appl. Catal. A*, Vol. 268 (2004):207-216.
- [18] Ma L., Trimm D.L., Jiang C., "The design and testing of an auto-thermal reactor for the conversion of light hydrocarbons to hydrogen-I: The kinetics of the catalytic oxidation of light hydrocarbons", *Appl. Catal. A*, Vol. 138 (1996): 275–283.
- [19] Reid R.C., Prausnitz J.M., Poling B.E., "The Properties of Gases and Liquids", McGraw-Hill, New York, 1988.
- [20] Rostrup-Nielsen J. R., "Catalytic steam reforming", *Catalysis, Science and Technology*, Springer Verlag, Berlin, chapter 1, Vol. 5 (1984):1-117.
- [21] Rostrup-Nielsen, J.R., "Conversion of hydrocarbons and alcohols for fuel cells." *Physical Chemistry Chemical Physics (PCCP)*, Vol. 3 (2001):283-288.
- [22] Scognamiglio D., Russo L., Maffettone P.L., Salemm L., Simeone M., Crescitelli S., "Modelling and simulation of a catalytic autothermal methane reformer with Rh catalyst." *Int. J. Hydrogen Energy*, Vol. 37 (2012):263-275.
- [23] Trimm D.L., Lam C.W., "The combustion of methane on platinum-alumina fibre catalysts—I. Kinetics and mechanism", *Chem. Eng. Sci.*, Vol. 35 (1980): 1405–1413.
- [24] Xiu G., Li P., A. Rodrigues, "Sorption enhanced reaction process with reactive regeneration", *Chem. Eng. Sci.*, Vol. 57 (2002): 3893–3908.
- [25] Xu J., Froment G.F., "Methane steam reforming, methanation and water-gas shift: I. intrinsic kinetics", *AIChE J.*, Vol. 35 (1989): 88–96.
- [26] Yagi S., Kunii D., Wakao N., "Studies on axial effective thermal conductivities in packed beds", *AIChE J.*, Vol. 6 (1960): 543–546.
- [27] ZahediNezhad M., Rowshanzamir S., Eikani M.H., "Autothermal reforming of methane to synthesis gas: modeling and simulation." *Int. J. Hydrogen Energy*, Vol. 34 (2009) 1292-1300.